iDECON 2010 – International Conference on Design and Concurrent Engineering
Universiti Teknikal Malaysia Melaka (UTeM)
20-21 September 2010

Rollover Prevention System for Passenger Vehicle

Mochamad Safarudin[1*], Amrik Singh[1], and Haeryip Sihombing[2]
[1]Faculty of Mechanical Engineering,
University Teknikal Malaysia Melaka, Durian Tunggal, 76109 Melaka, Malaysia
[2]Faculty of Manufacturing Engineering,
University Teknikal Malaysia Melaka, Durian Tunggal, 76109 Melaka, Malaysia
*corresponding author: andims@utem.edu.my

Abstract – An active roll control using roll moment rejection algorithm based on 14 DOF full vehicle model is proposed in this paper. For tire model, the Magic Tire formula was used. The full vehicle model was simulated and compared with vehicle dynamics simulation software and validated using an instrumented experimental vehicle. The active roll control algorithm was then introduced to the vehicle model. Combined with PID control, the results were then simulated and analyzed. From the simulation, it was found that the algorithm can significantly reduce the roll angle and roll rate of the vehicle and eventually prevent the vehicle from rollover. The improvement of the roll motion also reduces the load transfer from the inner wheels to outer wheels and hence increases the road holding during cornering.

Keywords – Active roll control, PID control, Magic Formula, 14 DOF full vehicle model

I. INTRODUCTION

Various types of electronic control systems have been actively employed in automotive applications to improve vehicle handling and passenger safety [5]. Active suspension was introduced to provide solution between conflict requirement between ride and handling. Although active suspension research have been carried out for years, most of the studies focuses on the ride comfort and very few of the researchers concentrated on the improvement of the vehicle handling using active suspension. Active roll control is an example of active suspension used to improve vehicle handling and passenger safety.

During cornering, the roll moment causes the normal load transfer from inner wheels to outer wheels. This load transfer strongly influences the lateral vehicle dynamics. Due to non-linear properties of pneumatics tires, the total lateral force capability of front or rear axle decreases as a result of load transfer. To overcome this problem, an active roll control system is introduced to reduce load transfer during cornering. Active roll control system enables the modulation the normal force at each corner of the vehicle body and hence it is capable of reducing vehicle body roll motion.

The objective of this paper is to investigate the performance of active roll control system in reducing vehicle body roll motion and hence preventing vehicle rollover.

II. VEHICLE MODELING

Shim [8] presented a comprehensive 14 DOF vehicle model which includes the dynamics of the roll center to study the roll behavior of the vehicle. The tire model used was the Magic Formula tire model. Step steer, ramp steer, and J-turn inputs were given to the vehicle model for validation purpose. The limitation, simplified equation validity and assumption of various modeling was discussed by analyzing their effect on the model roll response for step steer, ramp steer and J turn test. This paper presented development of 14 DOF vehicle model and implementation of active roll control structure on the validated vehicle model. This 14-DOF vehicle model was used by researchers in references [3], [6], and [8] in predicting the dynamic behavior of the vehicle.

A. Vehicle Model

The 14 DOF vehicle model shown in Fig. 1 is sufficient to study the dynamic behavior of the vehicle in longitudinal, lateral, and vertical direction. This model is made up of a sprung mass and four unsprung masses. The vehicle body has 6 DOF which are translational motions in x, y, and z direction and angular motions about those three axes. Roll, pitch and yaw motions are the rotation about x, y, and z axes respectively. Each of the wheels has translational motion in z direction and wheel spin about y direction. Magic Formula tire model [4] is used to represent the longitudinal and lateral tire behavior.

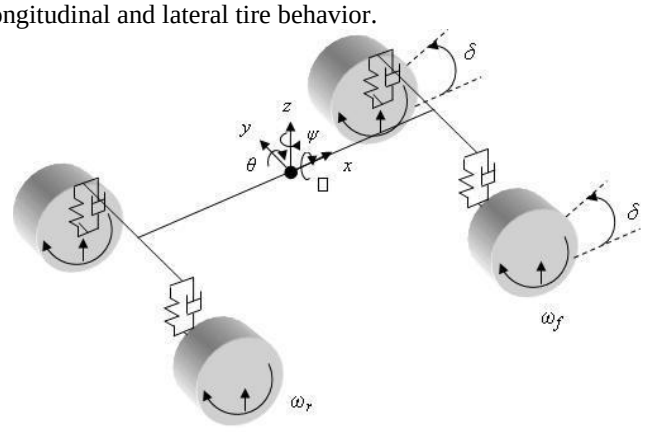

Fig. 1. 14 DOF Full Vehicle Model

B. Modeling Assumptions

The sprung and unsprung is represented using lumped mass [3]. The vehicle body is being modeled as rigid. The outer and inner wheel steer angle is assumed to be the same. The tires are assumed to having contact with the ground all the time. Aerodynamics effects are neglected. Roll center movement was not taken into account.

C. Ride Model

The 7 DOF ride model [6] as shown in Fig. 2 consists of sprung mass which is connected to four unsprung masses by the spring and damper at each corner. The sprung mass has 3 DOF that is the motion in z direction, and about x and y axes. The unsprung mass can only move in z direction.

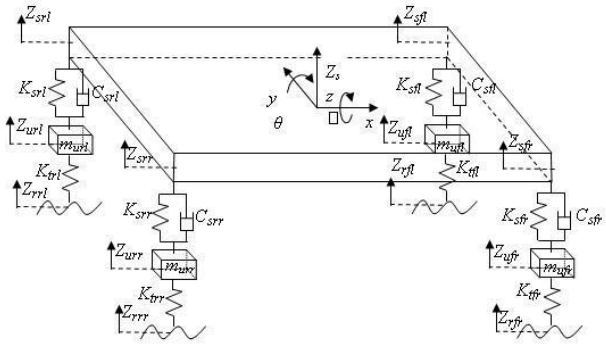

Fig. 2. 7 DOF Ride Model

Equation of motion for vertical forces:

$$F_{sfl} + F_{dfl} + F_{sfr} + F_{dfr} + F_{srl} + F_{drl} + F_{srr} + F_{drr} = m_s\ddot{Z}_s \quad (1)$$

Equation of motion for pitching moment:

$$(F_{srl} + F_{drl} + F_{srr} + F_{drr})b - (F_{sfl} + F_{dfl} + F_{sfr} + F_{dfr})a = I_p\ddot{\theta} \quad (2)$$

Equation of motion for rolling moment:

$$\left(F_{sfl} + F_{dfl} + F_{srl} + F_{drl}\right)\frac{w}{2} - \left(F_{sfr} + F_{dfr} + F_{srr} + F_{drr}\right)\frac{w}{2} = I_r\ddot{\phi} \quad (3)$$

Equation of motion for front left wheel vertical forces:

$$F_{tfl} - F_{sfl} - F_{dfl} = m_{ufl}\ddot{Z}_{ufl} \quad (4)$$

Equation of motion for front right wheel vertical forces:

$$F_{tfr} - F_{sfr} - F_{dfr} = m_{ufr}\ddot{Z}_{ufr} \quad (5)$$

Equation of motion for rear left wheel vertical forces:

$$F_{trl} - F_{srl} - F_{drl} = m_{url}\ddot{Z}_{url} \quad (6)$$

Equation of motion for rear right wheel vertical forces:

$$F_{trr} - F_{srr} - F_{drr} = m_{urr}\ddot{Z}_{urr} \quad (7)$$

The normal loads on each wheel are shown as following:

$$F_{zfl} = \frac{m_s gb}{2(a+b)} + m_{ufl}g + F_{fl}$$

$$F_{zfr} = \frac{m_s gb}{2(a+b)} + m_{ufr}g + F_{fr}$$

$$F_{zrl} = \frac{m_s ga}{2(a+b)} + m_{m_{url}}g + F_{rl}$$

$$F_{zrr} = \frac{m_s ga}{2(a+b)} + m_{urr}g + F_{rr} \quad (8)$$

D. Handling Model

The 7 DOF handling model [1] as shown in Fig. 3 has longitudinal, lateral and yaw motions at the vehicle body and wheel spin motion at each of the four wheels.

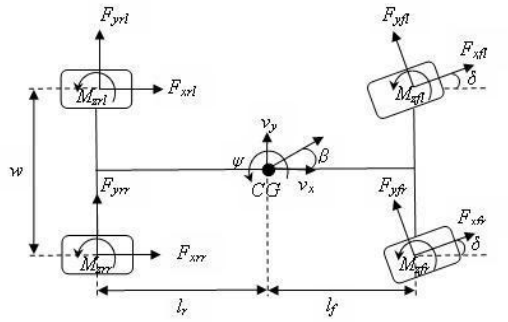

Fig. 3. 7 DOF Handling Model

There are two terms that contributes to the inertial longitudinal acceleration at the center of gravity of the vehicle, a_x namely the acceleration which is due to the motion along x axis, $\dot{v}_x$ and the centripetal acceleration, $v_y\dot{\psi}$.

$$a_x = \dot{v}_x - v_y\dot{\psi} \quad (9)$$

The longitudinal equation of motion is given by:

$$F_{xfl}cos\delta - F_{yfl}sin\delta + F_{xfr}cos\delta - F_{yfr}sin\delta + F_{xrl} + F_{xrr} = m_t a_x \quad (10)$$

Similarly, there are two terms that contributes to the inertial lateral acceleration at center of a_y, which is the inertial acceleration at the center of gravity of the vehicle is made up of two terms. The two terms are the acceleration which is due to the motion along y axis, $\dot{v}_y$ and the centripetal acceleration, $v_x\dot{\psi}$.

$$a_y = \dot{v}_y + v_x\dot{\psi} \quad (11)$$

The lateral equation of motion is given by:

$$F_{yfl}cos\delta + F_{xfl}sin\delta + F_{yfr}cos\delta + F_{xfr}sin\delta + F_{yrl} + F_{yrr} = m_t a_y \quad (12)$$

The front and rear slip angles equations are as follow:

$$\alpha_f = tan^{-1}\left(\frac{v_y + l_f\dot{\psi}}{v_x}\right) - \delta \quad (13)$$

$$\alpha_r = tan^{-1}\left(\frac{v_y - l_r\dot{\psi}}{v_x}\right) \quad (14)$$

Front tire longitudinal velocity required to obtain the longitudinal slip is defined as:

$$v_{wxf} = V_{tf}cos\alpha_f \quad (15)$$

where the speed of the front tire is given by the equation below.

$$V_{tf} = \sqrt{\left(v_y + l_f\dot{\psi}\right)^2 + v_x^2} \quad (16)$$

Rear tire longitudinal velocity required to obtain the longitudinal slip is defined as:

$$v_{wxr} = V_{tr}cos\alpha_r \quad (17)$$

where the speed of the rear tire is given by the following equation.

$$V_{tr} = \sqrt{\left(v_y - l_r\dot{\psi}\right)^2 + v_x^2} \quad (18)$$

The front and rears wheel longitudinal slip under braking condition is defined as follow:

$$S_{af} = \frac{v_{wxf} - \omega_f R_w}{v_{wxf}} \quad (19)$$

$$S_{ar} = \frac{v_{wxr} - \omega_r R_w}{v_{wxr}} \quad (20)$$

The summation of yawing moment is given by:

$$J_z\ddot{\psi} = [-\frac{w}{2}F_{xfl}cos\delta + \frac{w}{2}F_{xfr}cos\delta - \frac{w}{2}F_{xrl} + \frac{w}{2}F_{xrr} + \frac{w}{2}F_{yfl}sin\delta - \frac{w}{2}F_{yfr}sin\delta + l_fF_{xfl}sin\delta + l_fF_{yfl}cos\delta + l_fF_{xfr}sin\delta + l_fF_{yfr}cos\delta - l_rF_{yrl} - l_rF_{yrr} + M_{zfl} + M_{zfr} + M_{zrl} + M_{zrr}] \quad (21)$$

The acceleration of the vehicle in x direction as shown in Fig. 4 causes the pitching moment whereas the acceleration in the y direction contributes to the rolling moment as shown in Fig. 5. Summation of pitching moment about the y-axis is as follow:

$$I_{sy}\ddot{\theta} = m_s a_x h + m_s g h\theta - k_\theta\theta - \beta_\theta\dot{\theta} \quad (22)$$

Summation of rolling moment about the x-axis is given as follow:

$$(I_r + m_s(h - h_{rc})^2)\ddot{\phi} = m_s a_y(h - h_{rc})cos\phi + m_s g(h - h_{rc})sin\phi - k_\phi\phi - \beta_\phi\dot{\phi} \quad (23)$$

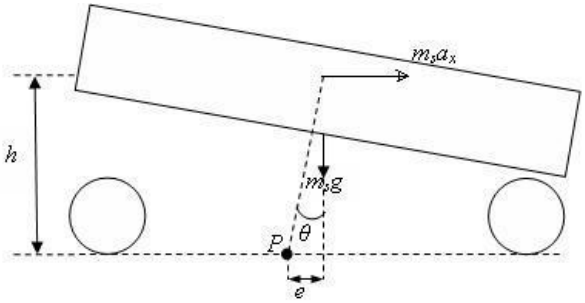

Fig. 4. Pitching Moment

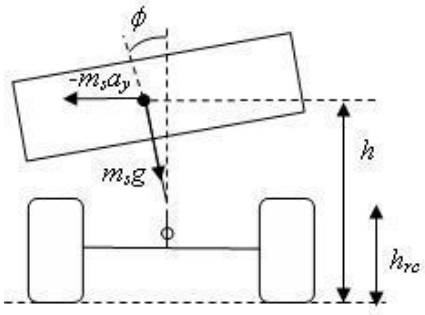

Fig. 5. Rolling Moment

The equation of motion of each wheel spin based on the diagram in Fig.6 is given as below.

$$I_w\dot{\omega}_{fl} = T_{dfl} - T_{bfl} - F_{xfl}R_w$$
$$I_w\dot{\omega}_{fr} = T_{dfr} - T_{bfr} - F_{xfr}R_w$$
$$I_w\dot{\omega}_{rl} = T_{drl} - T_{brl} - F_{xrl}R_w$$
$$I_w\dot{\omega}_{rr} = T_{drr} - T_{brr} - F_{xrr}R_w \quad (24)$$

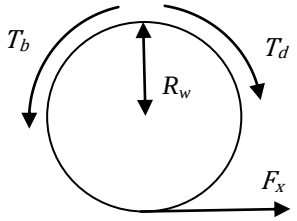

Fig. 6. Wheel Spin Motion under Throttle and Brake Inputs

III. SIMULATION AND VALIDATION OF MODEL

For 14 DOF vehicle model validation purpose, 180 degrees step steer at 35 kph and double lane change at 80 kph tests were conducted using an instrumented vehicle. For simulation purpose, the steering wheel angles for both of the test were taken from the steering wheel sensor as shown in Fig. 7. Accelerometer was used to measure the lateral acceleration, gyro-sensors to measure the yaw and roll rates, and vehicle speed sensor to measure the longitudinal speed of the vehicle. The 14 DOF vehicle model was validated using practical experimental data which was obtained from the experiment conducted by the Smart Material and Automotive Control Lab of Universiti Teknikal Malaysia Melaka.

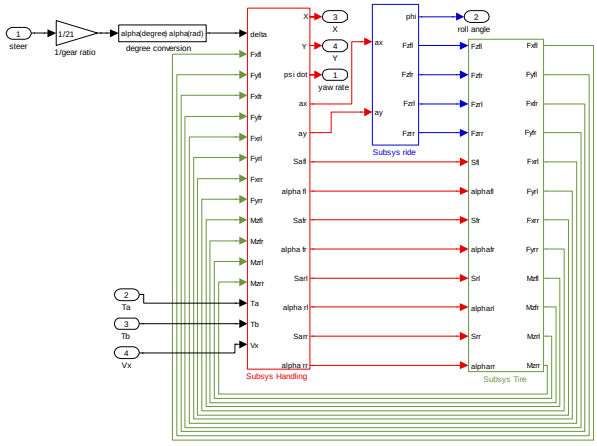

Fig. 7. 14 DOF Vehicle Model in SIMULINK

The output responses that were analyzed for those tests were the vehicle body yaw rate, lateral acceleration, and roll angle and tire slip angle. The difference in terms of the trend and magnitude between the simulation and the experimental results was discussed.

IV. ACTIVE ROLL CONTROL SUSPENSION SYSTEM CONTROLLER STRUCTURE

The control structure of active roll control system shown in Fig. 8 consists of inner loop controller that rejects the roll motion due to the weight transfer, outer loop that stabilize the roll response and input decoupling transformation that combines inner and outer control loop.

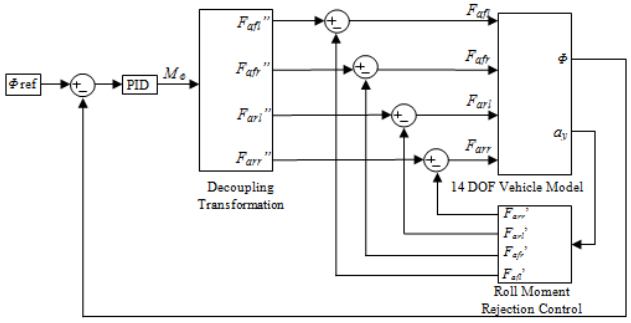

Fig. 8. Control Structure of ARC System

There are four control input forces F_{afl}, F_{afr}, F_{arl}, and F_{arr} which can be the hydraulic or pneumatic actuator forces. The equivalent forces for heave, pitch and roll are given by:

$$F_z = F_{afl}" + F_{afr}" + F_{arl}" + F_{arr}"$$
$$M_\theta = -F_{afl}"a - F_{afr}"a + F_{arl}"b + F_{arr}"b$$
$$M_\phi = F_{afl}"(0.5w) - F_{afr}"(0.5w) + F_{arl}"(0.5w) - F_{arr}"(0.5w) \quad (25)$$

Matrix form representation of the above equations is shown below.

$$\begin{bmatrix} F_z \\ M_\theta \\ M_\phi \end{bmatrix} = \begin{bmatrix} 1 & 1 & 1 & 1 \\ -a & -a & b & b \\ 0.5w & -0.5w & 0.5w & -0.5w \end{bmatrix} \begin{bmatrix} F_{afl}" \\ F_{afr}" \\ F_{arl}" \\ F_{arr}" \end{bmatrix}$$

For a linear system of equation $y = Dx$ if $D \in \Re^{m \times n}$ has full row rank, then it has right inverse D^{-1} such that $DD^{-1} = I^{m \times m}$. Using $D^{-1} = D^T(DD^T)^{-1}$. The inverse relationship can be expressed as:

$$\begin{bmatrix} F_{afl}" \\ F_{afr}" \\ F_{arl}" \\ F_{arr}" \end{bmatrix} = \begin{bmatrix} \frac{b}{2(a+b)} & \frac{-1}{2(a+b)} & \frac{1}{2w} \\ \frac{b}{2(a+b)} & \frac{-1}{2(a+b)} & -\frac{1}{2w} \\ \frac{a}{2(a+b)} & \frac{1}{2(a+b)} & \frac{1}{2w} \\ \frac{a}{2(a+b)} & \frac{1}{2(a+b)} & -\frac{1}{2w} \end{bmatrix} \begin{bmatrix} F_z \\ M_\theta \\ M_\phi \end{bmatrix}$$

As shown in Fig. 8, PID controller is used for outer controller to stabilize roll response. During cornering, lateral force acts at the body center of gravity and hence causes roll moment on the body. The inner loop controller determines amount of the actuator forces required to create a moment which is equal in magnitude but opposite in direction of the roll moment. The roll moment is given by:

$$M_{roll} = m_s a_y h \quad (26)$$

Actuators are installed on each corner of the vehicle body to produce force that will oppose the roll motion of the vehicle body. Only two actuators on the outside wheel will produce force to counter the roll moment whereas the actuators on the inner wheels will be set to zero. The actuator force required to counter the roll moment for counter clockwise steering input is given by:

$$F_{afr}' = F_{arr}' = \frac{m_s a_y h}{w} \text{ and } F_{afl}' = F_{arl}' = 0 \quad (27)$$

For clockwise steering input, the actuator force required is given by:

$$F_{afl}' = F_{arl}' = \frac{m_s a_y h}{w} \text{ and } F_{afr}' = F_{arr}' = 0 \quad (28)$$

where

F_{afl}'= front left target force by inner loop controller
F_{afr}'= front right target force by inner loop controller
F_{arl}'= rear left target force by inner loop controller
F_{arr}'= rear right target force by inner loop controller

Subtracting the target force produced by the inner loop controller from the respective target force produced by the outer loop controller gives the ideal target force for each actuator as:

$$F_{afl} = F_{afl}" - F_{afl}'$$
$$F_{afr} = F_{afr}" - F_{afr}'$$
$$F_{arl} = F_{arl}" - F_{arl}'$$
$$F_{arr} = F_{arr}" - F_{arr}' \quad (29)$$

V. RESULT AND DISCUSSION

A. 180 degrees Step Steer Test at 35 kph

The step steer was performed using an instrumented vehicle for 180 degrees step steer angle at a speed of 35 kph. The steering wheel angle input for this test which is obtained from the steering wheel sensor is shown in Fig. 9.

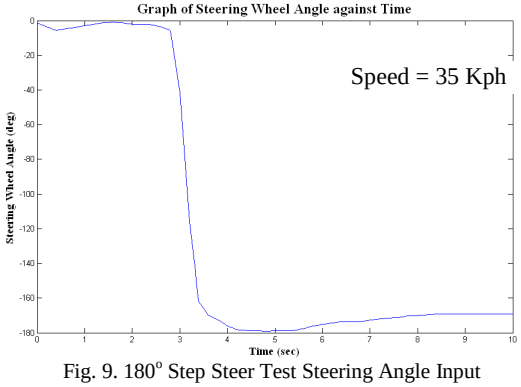

Fig. 9. 180° Step Steer Test Steering Angle Input

The Fig. 10 to 14 show the results of step steer simulation and the experimental results have similar trend between the simulation and experiment with slight difference in the magnitude due to some errors. Modeling simplification is the main source of the differences.

In terms of lateral acceleration and yaw rate as shown in Fig. 10 and 11 respectively, the simulation results follow the experiment results quite closely.

Fig. 12 presents the roll angle response whereby the simulation roll angle has similar trend with experiment roll angle but there is difference in the magnitude. The difference in magnitude is due to simplification done in the vehicle modeling. Anti-roll bar which greatly influences the roll angle of the vehicle body was not included in the vehicle modeling.

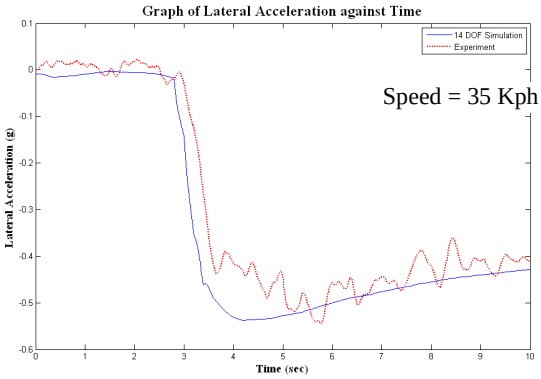

Fig. 10. 180° Step Steer Lateral Acceleration Response

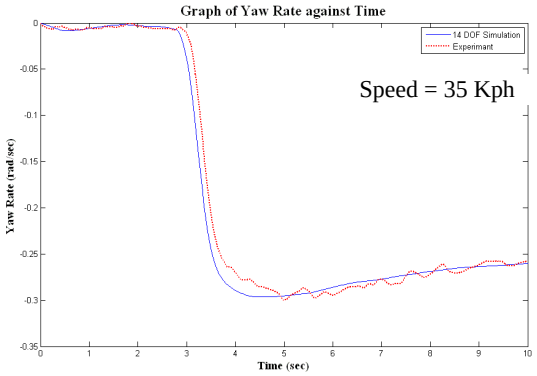

Fig. 11. 180° Step Steer Test Yaw Rate Response

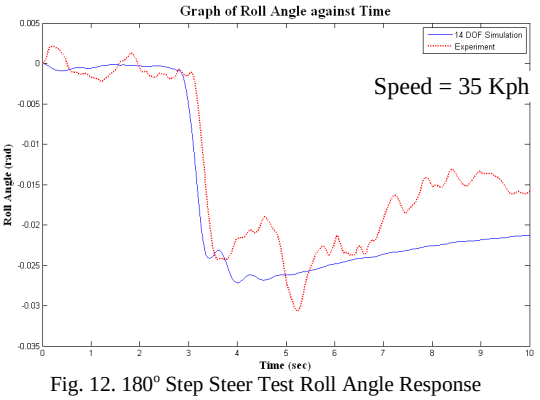

Fig. 12. 180° Step Steer Test Roll Angle Response

The tire slip angle responses of the front and rear right tires are shown in Fig. 13 and 14 respectively. From all the slip angle responses, experimental slip angle responses have higher magnitude than that of simulation especially for transient state. The magnitude difference is due to the difficulty in maintaining constant speed during the experiment whereas in simulation, a constant speed was given to the model.

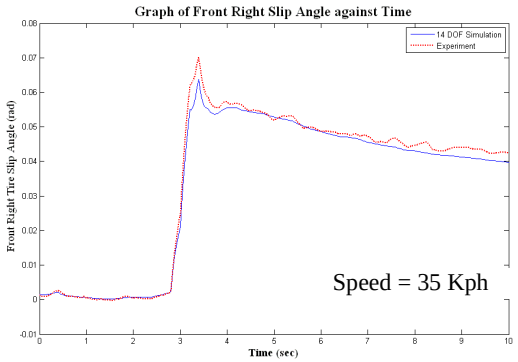

Fig. 13. 180° Step Steer Test Front Right Tire Slip Angle

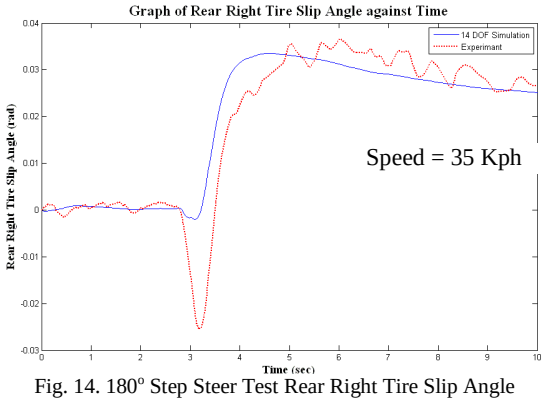

Fig. 14. 180° Step Steer Test Rear Right Tire Slip Angle

B. Double Lane Change Test at 80 kph

The double lane change maneuver at 80 kph was performed using the instrumented vehicle. For simulation, the steering angle input as shown in Fig. 15 was taken from the steering wheel sensor.

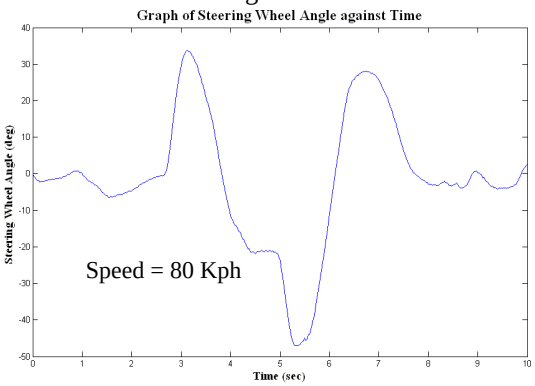

Fig. 15. Double Lane Change Test Steering Wheel Angle Input

The double lane change simulation and experimental results are presented in Fig. 16 to 20. The lateral acceleration and yaw rate results for both simulation and experiment are shown in Fig. 16 and 17 respectively. As shown, the simulation lateral acceleration and yaw rate matches very well with the experimental results.

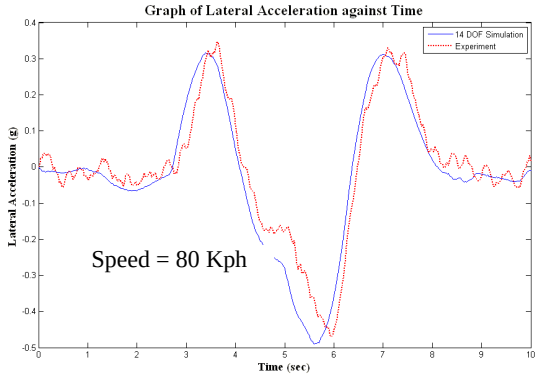

Fig. 16. Double Lane Change Test Lateral Acceleration Response

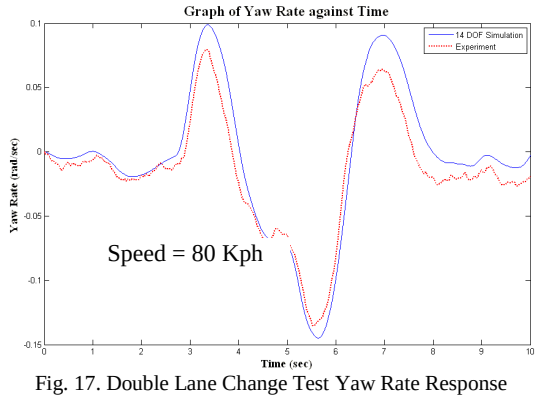

Fig. 17. Double Lane Change Test Yaw Rate Response

The simulation and experimental roll angle results for double lane change maneuver at 80 kph is shown in Fig. 18. Again, trend of both simulation and experimental roll angle is similar but slightly differs in magnitude due to the vehicle modeling simplifications such as ignoring the anti-roll bar effect.

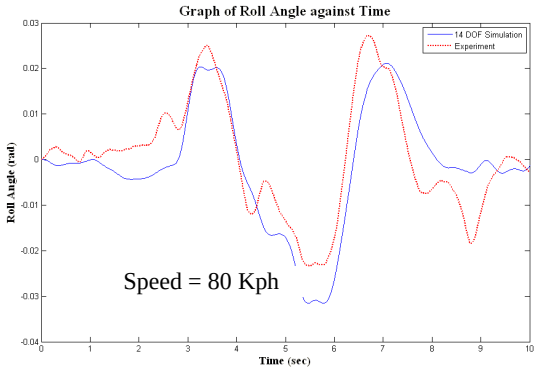

Fig. 18. Double Lane Change Test Roll Angle Response

Front right and rear right tire slip angle responses are shown in Fig. 19 and 20 respectively. The trends of the simulation for front and rear tire slip angles results agrees with the experiment tire slip angle results. Difficulty in maintaining a constant speed throughout the maneuver contributes to the difference in magnitude.

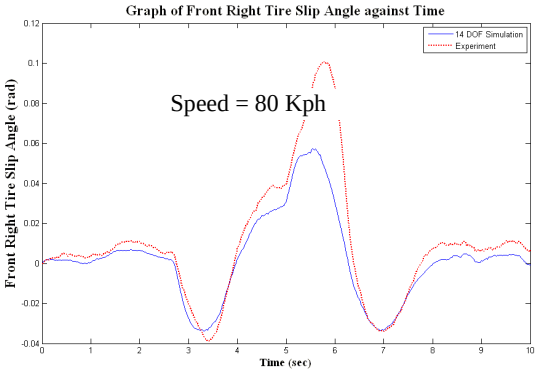

Fig. 19. Double Lane Change Test Front Right Tire Slip Angle

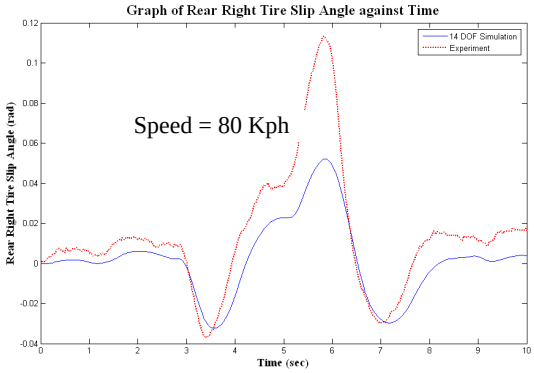

Fig. 20. Double Lane Change Test Rear Right Tire Slip Angle

C. Simulation ARC Performance for Step Steer Test

For 180 degrees step steer test, the steering wheel angle input was given to the model using a signal builder in SIMULINK.

Fig. 21 shows the roll rate response at the body center of gravity of the vehicle for the 180 degrees step steer test at a speed of 50 kph for passive suspension system, PID control without the roll moment rejection loop and PID control with roll moment rejection loop. Step steer test is carried out to study the transient response under steering input. It can be seen that the PID control without the roll moment rejection loop reduces the vibratory motion of the vehicle and PID control with roll moment rejection loop significantly reduces the roll rate of the vehicle. In transient state, the PID control with roll moment rejection loop and PID control without roll moment rejection loop reduces the percentage of the overshoot compared to the passive suspension system. PID control with roll moment rejection loop reduces the percentage of the overshoot even better than the PID control without roll moment rejection loop. In the steady state, the PID control with roll moment rejection loop shows slightly improves the settling time compared to the PID control without the roll moment rejection loop.

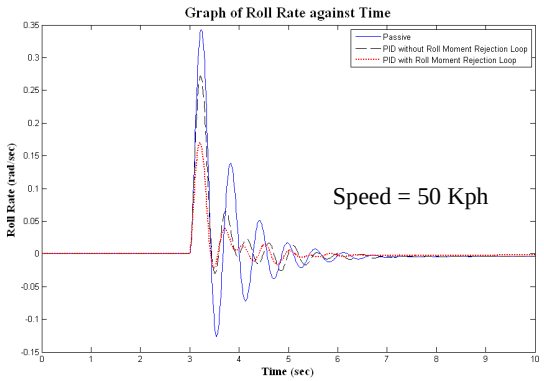

Fig. 21. Roll Rate Response for ARC Performance during 180° Step Steer Test at 50 kph

The roll angle response at the body center of gravity of the vehicle for the 180 degrees step steer test at a speed of 50 kph for passive suspension system, PID control without the roll moment rejection loop and PID control with roll moment rejection loop is presented in Fig. 22. As shown in the Fig. 22, the PID control without roll moment rejection loop reduces the body vibratory motion whereas the PID control with the roll moment rejection loop drastically reduces the roll angle of the vehicle body. Reduced body lean during cornering decreases the tendency for rollover. The improvement of the roll motion also reduces the load transfer from the inner wheels to outer wheels and hence increases the road holding during cornering.

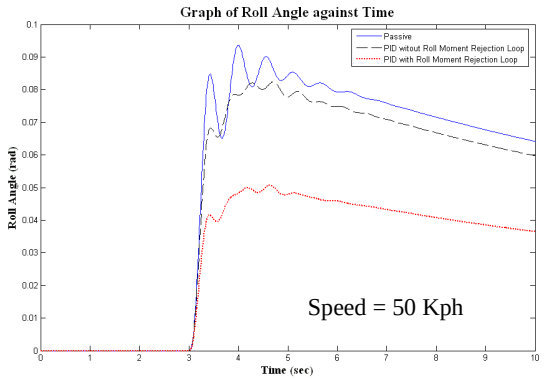

Fig. 22. Roll Angle Response for ARC Performance during 180° Step Steer Test at 50 kph

D. Simulation ARC Performance for Double Lane Change Test

For double lane change maneuver, the steering wheel angle input was taken from CarSimEd software at vehicle speed of 80 kph.

Fig. 23 shows the roll rate response at the body center of gravity of the vehicle for the double lane change test at a speed of 80 kph for passive suspension system, PID control without the roll moment rejection loop and PID control with roll moment rejection loop. A double lane change is often used in avoiding obstacles in an emergency. As shown in the Fig. 23, the PID control without roll moment rejection loop shows slight improvement in roll rate response and PID control with roll moment rejection loop shows significant improvement in reducing the roll rate response compared to passive suspension system.

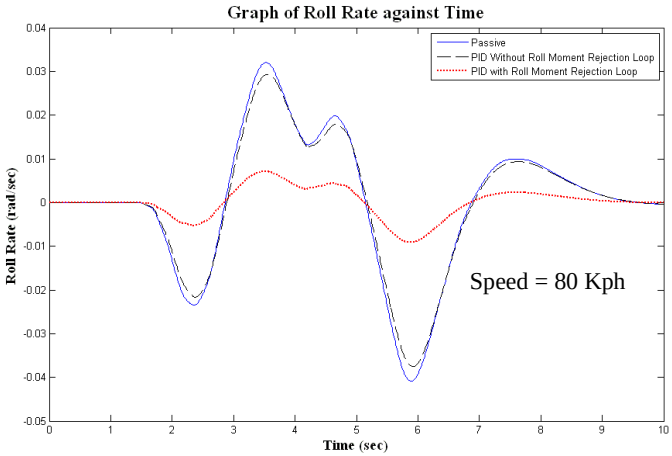

Fig. 23. Roll Rate Response for ARC Performance during Double Lane Change Test at 80 kph

The vehicle body roll angle at body center of gravity for double lane change maneuver at 80 kph for PID control with roll moment rejection loop, PID control without roll moment rejection loop is shown in the Fig. 24. It is clearly shown that the PID control without roll moment rejection loop slightly improves the roll angle of the body and PID control with roll moment rejection loop extensively reduces the roll angle during double lane change maneuver. So it is proven that ARC can significantly reduce the roll motion of the vehicle and hence improve the maneuverability of the vehicle when extensive steering input is given by the driver.

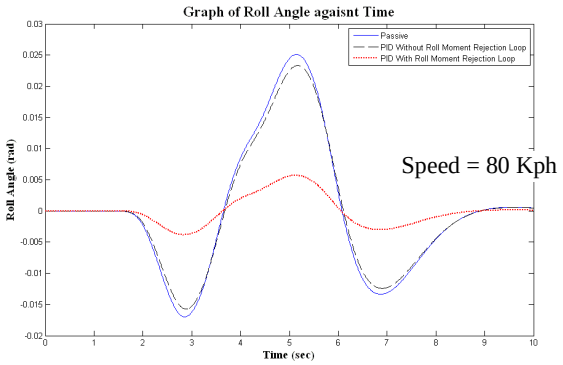

Fig. 24. Roll Angle Response for ARC Performance during Double Lane Change Test at 80 kph

VI. CONCLUSION

A 14 DOF vehicle model which includes ride model, handling, and tire model was developed. The 14 DOF vehicle model was validated with instrumented vehicle for 180 degrees step steer test at 35 kph and double lane change at 80 kph. The 14 DOF vehicle model was validated for lateral acceleration, yaw rate, roll angle and tire slip angle responses. The 14 DOF model validation results show the trend between the simulation and experiment was similar with small difference in the magnitude. The difference arises due to the vehicle

model simplification such as ignoring anti-roll bar, body flexibility, and movement of roll center.

The effect of the active roll control in improving the roll rate and roll angle for step steer and double lane change maneuvers were studied. For both 180 degrees step steer test at 50 kph and double lane change test at 80 kph, PID with roll moment rejection loop shows very significant improvement in terms of roll angle and roll rate responses, and followed by PID without roll moment rejection loop which shows slight improvement compared to passive vehicle. It is proven that the active roll control has the capability in reducing the roll motion of the vehicle and hence reduces the tendency to rollover. ARC also reduces the load transfer during cornering and therefore improves the road holding under extensive steering input.

REFERENCES

[1] Blundell, M. & Harty, D. (2004). *The Multibody Systems Approach to Vehicle Dynamics*.1st Ed. Warrandale, PA: Society of Automotive Engineering Inc.

[2] Gilispie, T. (1992). *Fundamental of Vehicle Dynamics*. Warrandale, PA: Society of Automotive Engineering Inc.

[3] Hudha, K., Kadir, Z. A., Said, M. R. & Jamaluddin, H. (2008). *Modeling, Validation, and Roll Moment Rejection Control of Pneumatically Actuated Active Control for Improving Vehicle Lateral Dynamics*. Int. J. Engineering Systems Modeling and Simulation.

[4] Pacejka, H. (2002). *Tire and Vehicle Dynamics*. 1st Ed. Warrandale, PA:Society of Automotive Engineering Inc.

[5] Rajamani, R. (2005) *Vehicle Dynamics and Control.* New York: Springer.

[6] Setiawan, J.D., Safarudin, M. & Singh, A. (2009). *Modeling, Simulation and Validation of 14 DOF Full Vehicle Model*. International Conference on Instrumentation, Communications, Information Technology, and Biomedical Engineering (ICICI-BME).

[7] Shim, T. & Ghike, C. (2005). *Understanding the Limitation of Different Vehicle Models for Roll Dynamics Studies*. Vehicle System Dynamics.

[8] Shim, T. & March, C. (2006). *Integrated Control of Suspension and Front Steering to Enhance Vehicle Handling*. Journal of Automobile Engineering.

APPENDIX

Vehicle Model Parameters:

Vehicle Parameters	Values
Sprung mass, m_s (kg)	920
Vehicle mass, m_t (kg)	1120
Front left/right unsprung mass, $m_{ufl} = m_{ufr}$ (kg)	50
Rear left/right unsprung mass, $m_{url} = m_{urr}$ (kg)	50
Sprung mass roll inertia, I_r (kgm^{-2})	400
Sprung mass pitch inertia, I_p (kgm^{-2})	2000
Sprung mass yaw inertia, J_z (kgm^{-2})	3190
Distance of sprung mass C.G. from front axle, a (m)	1.02
Distance of sprung mass C.G. from front axle, b (m)	1.55
Track width, w (m)	1.34
Front left/right suspension stiffness, $K_{sfl} = K_{sfr}$ (Nm^{-1})	30000
Rear left/right suspension stiffness, $K_{srl} = K_{srr}$ (Nm^{-1})	30000
Front left/right suspension damping coefficient, $C_{sfl} = C_{sfr}$ (Nsm^{-1})	750
Front left/right suspension damping coefficient, $C_{sfl} = C_{sfr}$ (Nsm^{-1})	750
Tire stiffness, $K_{tfl} = K_{tfr} = K_{trl} = K_{trr}$ (Nm^{-1})	200000
Nominal tire radius, r_o (m)	0.285
Wheel roll inertia, I_w (kgm^{-2})	1

PID Controller Parameters:

K_p	K_i	K_d
6000	0.5	3500